

Indirect (source-free) integration method for EMRIs: waveforms from geodesic generic orbits and self-force consistent radial fall

Alessandro Spallicci¹

Luca Bonetti¹, Stéphane Cordier², Richard Emilion², Sylvain Jubertie³, Patxi Ritter^{1,2}

Sofiane Aoudia

Université d'Orléans

¹ Observatoire des Sciences de l'Univers,

Laboratoire de Physique et Chimie de l'Environnement et de l'Espace,

LPC2E, UMR CNRS 7328, 3A Av. Recherche Scientifique, 45071 Orléans, France

² Laboratoire de Mathématiques, Analyse, Probabilités, Modélisation,

MAPMO, UMR CNRS 7349, Rue de Chartres, 45067 Orléans, France

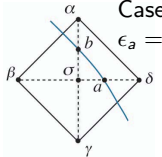
³ Laboratoire d'Informatique Fondamentale,

LIFO, EA 4022, Rue de Leonardo da Vinci, 45067 Orléans, France

22 May 2014

- ① The indirect (source-free) integration method.
 - Introduction by first order examples.
 - Geodesic waveforms at second order for generic orbits. Comparison with literature results.
- ② Self-force in Regge-Wheeler gauge. Pragmatic method.
 - Radial fall. Confirmations and dismissals.
- ③ Orbital evolution.
 - Self-consistency.
 - Differences in radial fall without and with self-consistent computation.

Indirect integration method: an example case

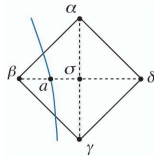
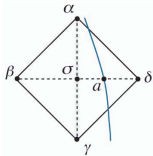
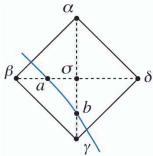


Case 1: particle crosses the $\beta - \delta$ line at a and $\gamma - \alpha$ line at b

$$\epsilon_a = \min \{a\delta, a\beta\}, \epsilon_b = \min \{b\alpha, b\gamma\}; \Psi_b^\pm = \Psi^\pm(t_b, r_b^*), \Psi_a^\pm = \Psi^\pm(t_a, r_a^*)$$

$$\Psi_\alpha^+ = \Psi_\beta^- - \Psi_\gamma^- + \Psi_\delta^+ - [\Psi]_a + [\Psi]_b - \epsilon_a [\Psi_{,r^*}]_a + \epsilon_b [\Psi_{,t}]_b + \mathcal{O}(h^2)$$

- No need of direct integration of the singular source
- Top cell value depending upon analytic expressions (and other cell's corners)



$$\Psi_\alpha^+ = \Psi_\beta^- - \Psi_\gamma^- + \Psi_\delta^+ - [\Psi]_a + [\Psi]_b - \epsilon_a [\Psi_{,r^*}]_a + \epsilon_b [\Psi_{,t}]_b + \mathcal{O}(h^2)$$

$$\Psi_\alpha^+ = \Psi_\beta^- - \Psi_\gamma^- + \Psi_\delta^+ - [\Psi]_a - \epsilon_a [\Psi_{,r^*}]_a + \mathcal{O}(h^2)$$

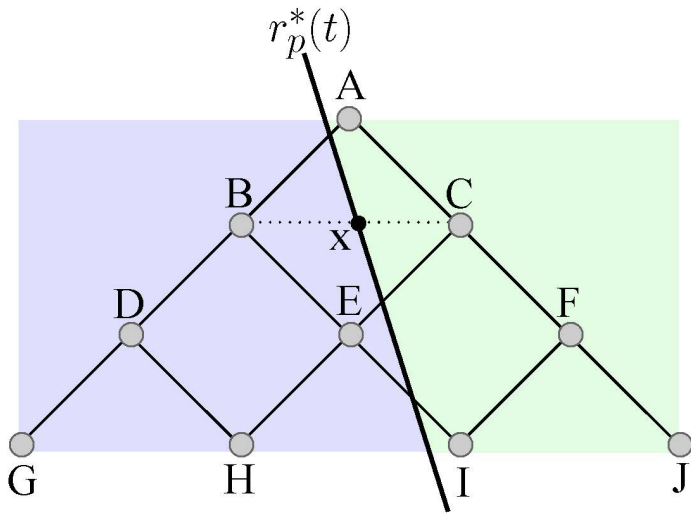
$$\Psi_\alpha^+ = \Psi_\beta^- - \Psi_\gamma^- + \Psi_\delta^+ + [\Psi]_a - \epsilon_a [\Psi_{,r^*}]_a + \mathcal{O}(h^2)$$

Use of jump conditions

- Haas (PRD 2007)
- Field, Hesthaven, Lau (CQG 2009)
- Barack, Sago (PRD 2010)
- Cañizares, Sopuerta (PRD 2009); Cañizares, Sopuerta, Jaramillo (2010)
- Aoudia, Spallicci (PRD 2011)

Fourth order stencil

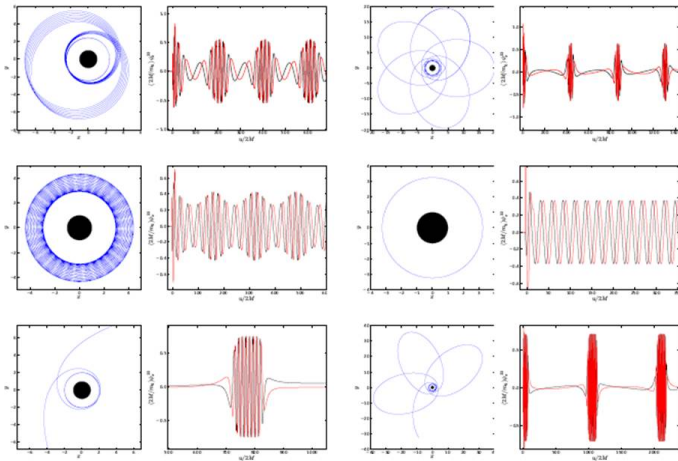
Ten points are need. Eight possible ways to cross the stencil.



1. Generic orbits: geodesic waveforms

Full agreement with previous results of other groups using other methods.

Numerical implementation



Geodesic waveforms: circular (energy)

ℓ	m	$\dot{E}_{\ell m}^{\infty}$	$\dot{E}_{\ell m}^{\infty}$ Poisson (1995,1997)	$\dot{E}_{\ell m}^{\infty}$ Martel 2004	$\dot{E}_{\ell m}^{\infty}$ Barack Lousto 2005	$\dot{E}_{\ell m}^{\infty}$ Sopuerta Laguna 2006
2	1	$8.1680 \cdot 10^{-07}$	$8.1633 \cdot 10^{-07}$ [0.06%]	$8.1623 \cdot 10^{-07}$ [0.07%]	$8.1654 \cdot 10^{-07}$ [0.03%]	$8.1662 \cdot 10^{-07}$ [0.02%]
2	2	$1.7064 \cdot 10^{-04}$	$1.7063 \cdot 10^{-04}$ [0.006%]	$1.7051 \cdot 10^{-04}$ [0.07%]	$1.7061 \cdot 10^{-04}$ [0.02%]	$1.7064 \cdot 10^{-04}$ [$< 0.001\%$]
3	1	$2.1757 \cdot 10^{-09}$	$2.1731 \cdot 10^{-09}$ [0.1%]	$2.1741 \cdot 10^{-09}$ [0.07%]	$2.1734 \cdot 10^{-09}$ [0.1%]	$2.1732 \cdot 10^{-09}$ [0.1%]
3	2	$2.5203 \cdot 10^{-07}$	$2.5199 \cdot 10^{-07}$ [0.02%]	$2.5164 \cdot 10^{-07}$ [0.2%]	$2.5207 \cdot 10^{-07}$ [0.01%]	$2.5204 \cdot 10^{-07}$ [0.002%]
3	3	$2.5471 \cdot 10^{-05}$	$2.5471 \cdot 10^{-05}$ [0.001%]	$2.5432 \cdot 10^{-05}$ [0.2%]	$2.5479 \cdot 10^{-05}$ [0.03%]	$2.5475 \cdot 10^{-05}$ [0.02%]
4	1	$8.4124 \cdot 10^{-13}$	$8.3956 \cdot 10^{-13}$ [0.2%]	$8.3507 \cdot 10^{-13}$ [0.7%]	$8.3982 \cdot 10^{-13}$ [0.2%]	$8.4055 \cdot 10^{-13}$ [0.08%]
4	2	$2.5099 \cdot 10^{-09}$	$2.5091 \cdot 10^{-09}$ [0.03%]	$2.4986 \cdot 10^{-09}$ [0.5%]	$2.5099 \cdot 10^{-09}$ [0.002%]	$2.5099 \cdot 10^{-09}$ [0.002%]
4	3	$5.7750 \cdot 10^{-08}$	$5.7751 \cdot 10^{-08}$ [0.001%]	$5.7464 \cdot 10^{-08}$ [0.5%]	$5.7759 \cdot 10^{-08}$ [0.02%]	$5.7765 \cdot 10^{-08}$ [0.03%]
4	4	$4.7251 \cdot 10^{-06}$	$4.7256 \cdot 10^{-06}$ [0.01%]	$4.7080 \cdot 10^{-06}$ [0.4%]	$4.7284 \cdot 10^{-06}$ [0.07%]	$4.7270 \cdot 10^{-06}$ [0.04%]
5	1	$1.2632 \cdot 10^{-15}$	$1.2594 \cdot 10^{-15}$ [0.3%]	$1.2544 \cdot 10^{-15}$ [0.7%]	$1.2598 \cdot 10^{-15}$ [0.3%]	$1.2607 \cdot 10^{-15}$ [0.2%]
5	2	$2.7910 \cdot 10^{-12}$	$2.7896 \cdot 10^{-12}$ [0.05%]	$2.7587 \cdot 10^{-12}$ [1.2%]	$2.7877 \cdot 10^{-12}$ [0.1%]	$2.7909 \cdot 10^{-12}$ [0.003%]
5	3	$1.0933 \cdot 10^{-09}$	$1.0933 \cdot 10^{-09}$ [$< 0.001\%$]	$1.0830 \cdot 10^{-09}$ [0.9%]	$1.0934 \cdot 10^{-09}$ [0.009%]	$1.0936 \cdot 10^{-09}$ [0.03%]
5	4	$1.2322 \cdot 10^{-08}$	$1.2324 \cdot 10^{-08}$ [0.01%]	$1.2193 \cdot 10^{-08}$ [1.1%]	$1.2319 \cdot 10^{-08}$ [0.03%]	$1.2329 \cdot 10^{-08}$ [0.05%]
5	5	$9.4544 \cdot 10^{-07}$	$9.4563 \cdot 10^{-07}$ [0.02%]	$9.3835 \cdot 10^{-07}$ [0.8%]	$9.4623 \cdot 10^{-07}$ [0.08%]	$9.4616 \cdot 10^{-07}$ [0.08%]
Total		$2.0293 \cdot 10^{-04}$	$2.0292 \cdot 10^{-04}$ [0.005%]	$2.0273 \cdot 10^{-04}$ [0.096%]	$2.0291 \cdot 10^{-04}$ [0.009%]	$2.0293 \cdot 10^{-04}$ [$< 0.001\%$]

Table: Circular orbit: energy flux $\dot{E}_{\ell m}$ values at infinity, for different ℓm modes and $\ell < 5$ (units of M^2/m_0^2). The semi-latus rectum is $p = 7.9456$. The first column lists our results, and the second those of Poisson (1995,1997), the third of Martel (2004), the fourth of Barack and Lousto (2005), the fifth of Sopuerta and Laguna (2006).

Geodesic waveforms: circular (angular momentum)

ℓ	m	$\dot{L}_{\ell m}^{\infty}$	$\dot{L}_{\ell m}^{\infty}$ Poisson (1995,1997)	$\dot{L}_{\ell m}^{\infty}$ Martel (2004)	$\dot{L}_{\ell m}^{\infty}$ Sopuerta Laguna
2	1	$1.8294 \cdot 10^{-5}$	$1.8283 \cdot 10^{-5}$ [0.06%]	$1.8270 \cdot 10^{-5}$ [0.1%]	$1.8289 \cdot 10^{-5}$ [0.03%]
2	2	$3.8218 \cdot 10^{-3}$	$3.8215 \cdot 10^{-3}$ [0.009%]	$3.8164 \cdot 10^{-3}$ [0.1%]	$3.8219 \cdot 10^{-3}$ [0.002%]
3	1	$4.8729 \cdot 10^{-8}$	$4.8670 \cdot 10^{-8}$ [0.1%]	$4.8684 \cdot 10^{-8}$ [0.09%]	$4.8675 \cdot 10^{-8}$ [0.1%]
3	2	$5.6448 \cdot 10^{-6}$	$5.6439 \cdot 10^{-6}$ [0.02%]	$5.6262 \cdot 10^{-6}$ [0.3%]	$5.6450 \cdot 10^{-6}$ [0.003%]
3	3	$5.7048 \cdot 10^{-4}$	$5.7048 \cdot 10^{-4}$ [< 0.001%]	$5.6878 \cdot 10^{-4}$ [0.2%]	$5.7057 \cdot 10^{-4}$ [0.02%]
4	1	$1.8841 \cdot 10^{-11}$	$1.8803 \cdot 10^{-11}$ [0.2%]	$1.8692 \cdot 10^{-11}$ [0.8%]	$1.8825 \cdot 10^{-11}$ [0.09%]
4	2	$5.6213 \cdot 10^{-8}$	$5.6195 \cdot 10^{-8}$ [0.03%]	$5.5926 \cdot 10^{-8}$ [0.5%]	$5.6215 \cdot 10^{-8}$ [0.003%]
4	3	$1.2934 \cdot 10^{-6}$	$1.2934 \cdot 10^{-6}$ [0.003%]	$1.2933 \cdot 10^{-6}$ [0.01%]	$1.2937 \cdot 10^{-6}$ [0.02%]
4	4	$1.0583 \cdot 10^{-4}$	$1.0584 \cdot 10^{-4}$ [0.01%]	$1.0518 \cdot 10^{-4}$ [0.6%]	$1.0586 \cdot 10^{-4}$ [0.03%]
5	1	$2.8293 \cdot 10^{-14}$	$2.8206 \cdot 10^{-14}$ [0.3%]	$2.8090 \cdot 10^{-14}$ [0.7%]	$2.8237 \cdot 10^{-14}$ [0.2%]
5	2	$6.2509 \cdot 10^{-11}$	$6.2479 \cdot 10^{-11}$ [0.05%]	$6.1679 \cdot 10^{-11}$ [1.3%]	$6.2509 \cdot 10^{-11}$ [0.001%]
5	3	$2.4487 \cdot 10^{-8}$	$2.4486 \cdot 10^{-8}$ [0.002%]	$2.4227 \cdot 10^{-8}$ [1.1%]	$2.4494 \cdot 10^{-8}$ [0.03%]
5	4	$2.7598 \cdot 10^{-7}$	$2.7603 \cdot 10^{-7}$ [0.02%]	$2.7114 \cdot 10^{-7}$ [1.8%]	$2.7613 \cdot 10^{-7}$ [0.05%]
5	5	$2.1175 \cdot 10^{-5}$	$2.1179 \cdot 10^{-5}$ [0.02%]	$2.0933 \cdot 10^{-5}$ [1.2%]	$2.1190 \cdot 10^{-5}$ [0.07%]
Total		$4.5449 \cdot 10^{-3}$	$4.5446 \cdot 10^{-3}$ [0.007%]	$4.5369 \cdot 10^{-3}$ [0.2%]	$4.5452 \cdot 10^{-3}$ [0.005%]

Table: Circular orbit: angular momentum flux $\dot{L}_{\ell m}$ values at infinity, for different ℓm modes and $\ell < 5$ (units of M/m_0^2). The semi-latus rectum is $p = 7.9456$. The first column lists our results, and the second those of Poisson (1995,1997), the third of Martel (2004), the fourth of Sopuerta and Laguna (2006).

Geodesic waveforms: elliptic (energy, angular momentum)

e	p	$\langle \dot{E}^\infty \rangle$	$\langle \dot{E}^\infty \rangle$ Cutler <i>et al.</i> (1994)	$\langle \dot{E}^\infty \rangle$ Martel (2004)	$\langle \dot{E}^\infty \rangle$ Sopuerta, Laguna (2006)
0.188917	7.50478	$3.1617 \cdot 10^{-4}$	$3.1680 \cdot 10^{-4}$ [0.2%]	$3.1770 \cdot 10^{-4}$ [0.5%]	$3.1640 \cdot 10^{-4}$ [0.07%]
0.764124	8.75455	$2.1026 \cdot 10^{-4}$	$2.1008 \cdot 10^{-4}$ [0.09%]	$2.1484 \cdot 10^{-4}$ [2.1%]	$2.1004 \cdot 10^{-4}$ [0.1%]

Table: Elliptic orbit: average of the energy flux (units of M^2/m_0^2), taken over a few periods in the case of two elliptic orbits $(e, p) = (0.188917, 7.50478)$ and $(0.764124, 8.75455)$. The differences with the results of Cutler *et al.* (1994), Martel (2004), and Sopuerta and Laguna (2006) are shown.

e	p	$\langle \dot{L}^\infty \rangle$	$\langle \dot{L}^\infty \rangle$ Cutler <i>et al.</i> (1994)	$\langle \dot{L}^\infty \rangle$ Martel (2004)	$\langle \dot{L}^\infty \rangle$ Sopuerta, Laguna (2006)
0.188917	7.50478	$5.9550 \cdot 10^{-3}$	$5.9656 \cdot 10^{-3}$ [0.2%]	$5.9329 \cdot 10^{-3}$ [0.4%]	$5.9555 \cdot 10^{-3}$ [0.008%]
0.764124	8.75455	$2.7531 \cdot 10^{-3}$	$2.7503 \cdot 10^{-3}$ [0.1%]	$2.7932 \cdot 10^{-3}$ [1.4%]	$2.7505 \cdot 10^{-3}$ [0.09%]

Table: Elliptic orbit: average of the angular momentum flux (units of M/m_0^2) taken over a few periods in the case of two elliptic orbits $(e, p) = (0.188917, 7.50478)$ and $(0.764124, 8.75455)$. The differences with the results of Cutler *et al.* (1994), Martel (2004), and Sopuerta and Laguna (2006) are shown.

Geodesic waveforms: elliptic (energy, angular momentum)

ℓ	$\langle \dot{E}_\ell^\infty \rangle$	$\langle \dot{E}_\ell^\infty \rangle$ Hopper, Evans (2010)	$\langle \dot{L}_\ell^\infty \rangle$	$\langle \dot{L}_\ell^\infty \rangle$ Hopper, Evans (2010)
2	$1.571333 \cdot 10^{-04}$	$1.57133846 \cdot 10^{-04}$ [0.0004%]	$2.092406 \cdot 10^{-03}$	$2.09219582 \cdot 10^{-03}$ [0.01%]
3	$3.776283 \cdot 10^{-05}$	$3.77696202 \cdot 10^{-05}$ [0.02%]	$4.745961 \cdot 10^{-04}$	$4.74663748 \cdot 10^{-04}$ [0.01%]
4	$1.149375 \cdot 10^{-05}$	$1.14987458 \cdot 10^{-05}$ [0.04%]	$1.399210 \cdot 10^{-04}$	$1.39978027 \cdot 10^{-04}$ [0.04%]
5	$3.837470 \cdot 10^{-06}$	$3.84046353 \cdot 10^{-06}$ [0.08%]	$4.575322 \cdot 10^{-05}$	$4.57886526 \cdot 10^{-05}$ [0.08%]
Total	$2.102273 \cdot 10^{-04}$	$2.10242676 \cdot 10^{-04}$ [0.007%]	$2.752676 \cdot 10^{-03}$	$2.75262625 \cdot 10^{-03}$ [0.002%]

Table: Elliptic orbit: average of the ℓ -mode energy (units of M^2/m_0^2) and angular momentum (units of M/m_0^2) fluxes radiated to infinity and taken over a few periods in the case of an elliptic orbit (e, p)=(0.764124, 8.75455). Each ℓ -mode is obtained by summing the flux over all the azimuthal m -modes such that $(\dot{E}_\ell^\infty, \dot{L}_\ell^\infty) = \sum_{m=-\ell}^{\ell} (\dot{E}_{\ell m}^\infty, \dot{L}_{\ell m}^\infty)$. The differences with the results of Hopper and Evans (2010) are shown.

Geodesic waveforms: parabolic (energy, angular momentum)

p	E^∞	E^∞	Martel (2004)	E^∞	Sopuerta, Laguna (2006)	E^{eh}	E^{eh}	Martel (2004)	E^{eh}	Sopuerta, Laguna (2006)
8.00001	3.5820	3.6703[2.4%]		3.5603[0.6%]		$1.8900 \cdot 10^{-1}$	$1.8876 \cdot 10^{-1}$	[0.1%]	$1.8884 \cdot 10^{-1}$	[0.008%]
8.001	2.2350	2.2809[2.0%]		2.2212[0.6%]		$1.1349 \cdot 10^{-1}$	$1.1260 \cdot 10^{-1}$	[0.8%]	$1.1339 \cdot 10^{-1}$	[0.09%]

Table: Parabolic orbit: energy radiated to infinity E^∞ , and to the horizon E^{eh} (units of M/m_0^2) for $p \simeq 8$. The differences with the results of Martel (2004), and Sopuerta and Laguna (2006) are shown.

p	L^∞	L^∞	Martel (2004)	L^∞	Sopuerta, Laguna (2006)	L^{eh}	L^{eh}	Martel (2004)	L^{eh}	Sopuerta, Laguna (2006)
8.00001	$2.9596 \cdot 10^1$	$3.0133 \cdot 10^1$	[1.8%]	$2.9415 \cdot 10^1$	[0.6%]	1.5137		1.5208[0.5%]		1.5112[0.2%]
8.001	$1.8813 \cdot 10^1$	$1.9088 \cdot 10^1$	[1.4%]	$1.8704 \cdot 10^1$	[0.6%]	$9.0964 \cdot 10^{-1}$	$9.1166 \cdot 10^{-1}$	[0.2%]	$9.0783 \cdot 10^{-1}$	[0.2%]

Table: Parabolic orbit: angular momentum radiated to infinity L^∞ , and to the horizon L^{eh} (units of $1/m_0^2$) for $p \simeq 8$. The differences with the results of Martel (2004), and Sopuerta and Laguna (2006) are shown.

Self-force on radial fall. Why.

- Classic problem.
- Lousto (2000) self-force is repulsive, divergence at the horizon, and ℓ dependency while Barack, Lousto (2001) self-force is attractive *but without analysis of the impact on the trajectory*.
- de Donder (harmonic) and Regge-Wheeler gauges: regular transformation (for radial only). The mode-sum regularisation is carried out entirely in RW gauge

$$F_{\text{self}}^{\alpha(\text{RW})} = \sum_{\ell=0}^{\infty} \left[F_{\text{ret}}^{\alpha\ell(\text{RW})} - A^{\alpha(\text{RW})} L - B^{\alpha(\text{RW})} - C^{\alpha(\text{RW})} L^{-1} \right] - D^{\alpha(\text{RW})}. \quad (1)$$

- Plunges and highly eccentric orbits much more frequent than expected (Amaro-Seoane's talk). IN THE LAST PART
- The most non-adiabatic orbit of all. Full justification for a self-consistent prescription.
- Very short orbit: hardly time for cumulative effects; does a self-consistent computation bring any difference?

The coordinate of the particle $\hat{r} = r + \Delta r$; 2nd order coordinate time derivative of the displacement is

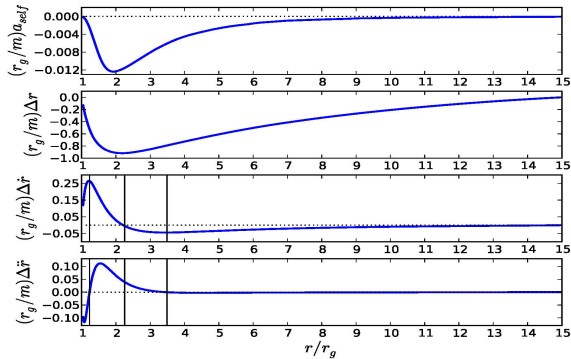
$$\Delta \ddot{r} = a_1(g_{\mu\nu}; r, \dot{r}) \Delta r + a_2(g_{\mu\nu}; r, \dot{r}) \Delta \dot{r} + a_{\text{self}}(h_{\mu\nu}; r, \dot{r}), \quad (2)$$

First two terms: background geodesic deviation (gd), a_{self} perturbation dependent term (coordinate time).

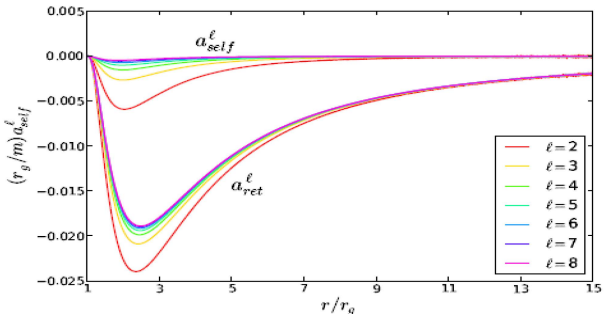
Pragmatic approach

Table: The four zones according to the sign of Δr , $\Delta \dot{r}$, $\Delta \ddot{r}$.

Zone	IV $r_g - 1.2 r_g$	III $1.2 r_g - 2.2 r_g$	II $2.2 r_g - 3.5 r_g$	I $3.5 r_g - r_0$
Δr	-	-	-	-
$\Delta \dot{r}$	+	+	-	-
$\Delta \ddot{r}$	-	+	+	-



Convergence of a_{self} , a_{ret}



Orbital evolution

The self-acceleration (MiSaTaQuWa-DeWh) term

$$\frac{D^2 \Delta z^\alpha}{d\tau^2} = -\underbrace{\frac{1}{2}(g^{\alpha\beta} + u^\alpha u^\beta)(2h_{\mu\beta;\nu}^{\text{tail}} - h_{\mu\nu;\beta}^{\text{tail}})u^\mu u^\nu}_{\text{Self-acceleration}} \quad (3)$$

(Already known) Equation presented at School on Mass and Capra Meeting (2008) in Orléans.

$$\frac{D^2 \Delta z^\alpha}{d\tau^2} = \underbrace{-R_{\mu\beta\nu}{}^\alpha u^\mu \Delta z^\beta u^\nu}_{\text{Background metric geodesic deviation}} - \underbrace{\frac{1}{2}(g^{\alpha\beta} + u^\alpha u^\beta)(2h_{\mu\beta;\nu}^{\text{tail}} - h_{\mu\nu;\beta}^{\text{tail}})u^\mu u^\nu}_{\text{Self-acceleration}} \quad (4)$$

- At late times Δz^α grows considerably.
- The equations of motion at n^{th} order perturbation theory are more accurate than the $(n-1)^{\text{th}}$ equations, but at late times the corrections at n^{th} order will become comparable to the corrections at $(n-1)^{\text{th}}$ order.
- The self-consistent prescription describes motion continuously corrected.

$e^x|_0 \sim 1 + x + \frac{x^2}{2}$ replaced by

$e^x|_0 \sim 1 \rightarrow e^x|_1 \sim e + e(x-1) \rightarrow e^x|_2 \sim e^2 + e^2(x-2)$ et caetera.

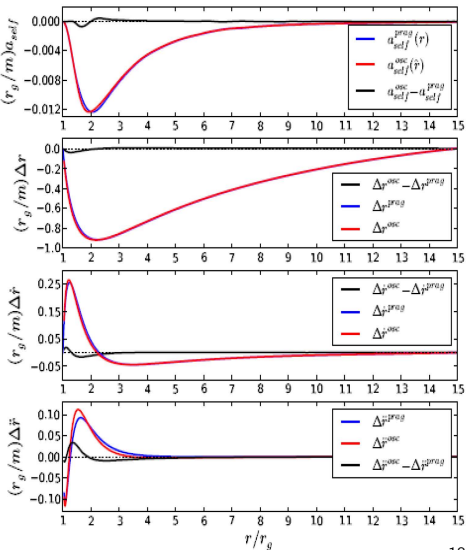
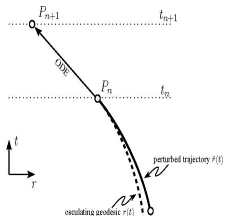
Orbital evolution: self-consistent prescription

$$\left\{ \begin{array}{l} \nabla^\gamma \nabla_\gamma \tilde{h}_{\alpha\beta} - 2R^\gamma{}_{\alpha\beta}{}^\delta \tilde{h}_{\gamma\delta} = -16\pi m u_\alpha(t) u_\beta(t) \frac{\delta^{(3)} [x^\mu - z_p^\mu(t)]}{\sqrt{-g}} \frac{d\tau}{dt} \\ u^\beta \nabla_\beta u^\alpha = -(g^{\alpha\beta} + u^\alpha u^\beta) (\nabla_\delta h_{\beta\gamma}^{\text{tail}} - \frac{1}{2} \nabla_\beta h_{\gamma\delta}^{\text{tail}}) u^\gamma u^\delta \\ h_{\alpha\beta}^{\text{tail}}(x) = m \int_{-\infty}^{\tau_{\text{ret}}} \left(G_{\alpha\beta\alpha'\beta'}^+ - \frac{1}{2} g_{\alpha\beta} G_{\gamma\alpha'\beta'}^{+\gamma} \right) [x, z_p(\tau')] u^{\alpha'} u^{\beta'} d\tau' \end{array} \right. \quad (5)$$

- The self-consistent approach can be applied at first order, as well as at higher orders. There isn't a conceptual impediment.
- Two ways to implement self-consistency: through stretches of osculating geodesics (the case here), or computing self-force quantities and mode-sum parameters on the 'real' non-geodesic trajectory (never done for a gravitational case).
- Though the background geodesic deviation loses relevance in a continuous correction approach, its presence is justified by discretisation (time slices) of the trajectory.

Pragmatic versus self-consistent (osculating)

a_{self} , Δr , $\Delta \dot{r}$, and $\Delta \ddot{r}$ from the pragmatic and self-consistent (osculating) methods, and their difference, for $r_0 = 15r_g$. The amplitudes, when computed self-consistently, differ of about 3% after $4r_g$, and the four zones are slightly shifted towards the horizon.



Production on low frequency sources

- Pierro V., Pinto I., Spallicci A., Laserra A., Recano F., 2001. *Fast and accurate computational tools for gravitational waveforms from binary systems with any orbital eccentricity*, Mon. Not. Roy. Astr. Soc., 325, 358, arXiv:gr-qc/0005044.
- Pierro V., Pinto I., Spallicci A., 2002. *Computation of hypergeometric functions for gravitationally radiating binary stars*, Mon. Not. Roy. Astr. Soc., 334, 855.
- **Spallicci A. Aoudia S., 2004.** *Perturbation method in the assessment of radiation reaction in the capture of stars by black holes*, Class. Q. Grav., 21, S563, arXiv:gr-qc/0309039.
- Chauvineau B., Spallicci A., Fournier J.-D., 2005. *Brans-Dicke gravity in the capture of stars by black holes: some asymptotic results*, Class. Q. Grav., 22, S457, arXiv:gr-qc/0412053.
- **Aoudia S., Spallicci A., 2011.** *A source-free integration method for black hole perturbations and self-force computation: Radial fall*, Phys. Rev. D, 83, 064029, arXiv:1008.2507 [gr-qc].
- Blanchet L., Spallicci A., Whiting B., 2011. *Mass and motion in general relativity*, Springer Series on Fundamental Theory of Physics.
- **Ritter P., Spallicci A., Aoudia S., Cordier S., 2011.** *Fourth order indirect integration method for black hole perturbations: even modes*, Class. Q. Grav., 28, 134012, arXiv:1102.2404 [gr-qc].
- Spallicci A., 2013. *On the complementarity of pulsar timing and space laser interferometry for the individual detection of supermassive black hole binaries*, Astrophys. J., 764, 187, arXiv:1107.5984 [gr-qc].
- Spallicci A., Ritter P., Aoudia S., 2014. *Self-force driven motion in curved spacetime*, to appear in Int. J. Geom. Meth. Mod. Phys., arXiv:1405.4155 [gr-qc].
- Spallicci A., Ritter P., 2014. *A fully relativistic radial fall*, submitted.
- **Ritter P., Spallicci A., Aoudia S., Cordier S., 2014.** *Indirect (source-free) integration method for EMRIs: geodesic generic orbits and self-force consistent radial fall*, in preparation.

Grazie